

Tempering Characteristics of Two Low-Alloy Steels Used for Naval Applications

D.K. Biswas, M. Venkatraman, C.S. Narendranath, and V.P. Deshmukh

Tempering characteristics of two high-strength low-alloy steels (HY-80 and HX-80) with carbon contents of 0.14 and 0.07%, respectively, have been investigated by transmission electron microscopic analysis. Mechanical properties such as hardness, and tensile and impact properties of these two steels were correlated with microstructural features. It was observed that the major factors contributing to the equivalent strength, better toughness, and weldability of microalloyed HX-80 steel compared to HY-80 steel include judicious selection of tempering temperature, lower carbon content, and finer grain size.

1. Introduction

THE properties of steel plate used for shipbuilding applications are the most demanding because of the critical requirements of high performance, reliability, and dependability. HY-80 steel quenched and tempered to a yield strength of 540 MPa has been traditionally used as structural material for naval applications. The high cost associated with the welding of this steel, particularly in relation to stringent preheat requirement to avoid hydrogen-induced cracking, has recently focused attention on the search for more easily weldable steel without compromising the strength and toughness possessed by HY-80 steel.^[1] Many plate products have, therefore, been developed with an improved combination of strength, toughness, and weldability. Microalloying with niobium, vanadium, or titanium has been used in combination with controlled rolling and cooling, which has contributed to stronger and tougher steels through grain refinement and precipitation hardening compared to traditional quenching and tempering routes for HY-80 steel. Various grades of copper-bearing HSLA steels, such as HSLA-80 and HSLA-100, are examples of this type of application.^[2]

Another approach to improve the weldability of quenched and tempered steel for shipbuilding applications is modification of alloy chemistry to lower carbon and other alloying elements, thereby reducing the carbon equivalent (CE) and optimizing the properties by thermomechanical processing. In this study, a similar steel, designated HX-80, which has a lower carbon equivalent, was subjected to different tempering treatments to determine the optimum heat treatment for obtaining properties equivalent to that of HY-80 steel. This steel exhibited the same strength and toughness as that of HY-80 steel, but with superior weldability (CE = 0.44 compared to that of 0.75

in HY-80 steel). Preheating was found to be unnecessary up to a certain thickness in this steel. Consequently, considerable cost savings has been realized in the fabrication of warships using this steel.

This article discusses the tempering characteristics of HX-80 steel and compares them with those of HY-80 steel. It further correlates microstructural features with mechanical properties. The strengthening mechanisms of these steels have been studied with the help of metallography, transmission electron microscopy, and X-ray diffraction techniques.

2. Experimental

The chemical compositions of the HY-80 and the HX-80 steel plate used in the present study are given in Table 1. The primary difference in the chemical composition of these two steels is the amount of carbon, nickel, chromium, and copper, and the presence of other microalloying elements. The carbon content of HY-80 steel is ~0.14%, whereas that of HX-80 is less than 0.07%. Tensile samples were made from 25-mm thick quenched and tempered plate with the tensile axis parallel to the rolling direction as per ASTM E-8. Charpy impact samples were made in the L-T direction as per ASTM E-23. All samples were normalized and thereafter austenitized at 880 °C for 1 h, water quenched, and then tempered at different temperatures (e.g., 200, 400, 575, and 675 °C) for 1 h. Microstructural characterization was carried out on these samples.

Tensile tests were carried out at room temperature at a crosshead speed of 0.05 cm/min. From tension test results, yield strength, tensile strength, and ductility in terms of reduction in area were obtained. Impact testing was carried out using standard Charpy V-notch samples in a 358-J Tinius Olsen Model 74 instrumented impact testing machine. Microstructural characterization by transmission electron microscopy (TEM) was performed on the as-quenched specimens, as well as on the quenched and tempered specimens, of both HX-80

D.K. Biswas, M. Venkatraman, C.S. Narendranath, and V.P. Deshmukh, Naval Chemical and Metallurgical Laboratory, Defence R & D Organization, Naval Dockyard, Tiger Gate, Bombay, India.

Table 1 Typical Chemical Composition of HY-80 and Experimental Steel

Alloy	Composition, wt%											
	C	P	Mn	Si	S	Ni	Cr	Mo	Cu	Al	Nb	V
HY-80.....	0.15	0.014	0.26	0.23	0.003	2.65	1.55	0.38	0.010	0.050	nil	nil
HX-80.....	0.07	0.012	0.44	0.23	0.005	1.81	0.44	0.29	0.40	...	0.015	0.03

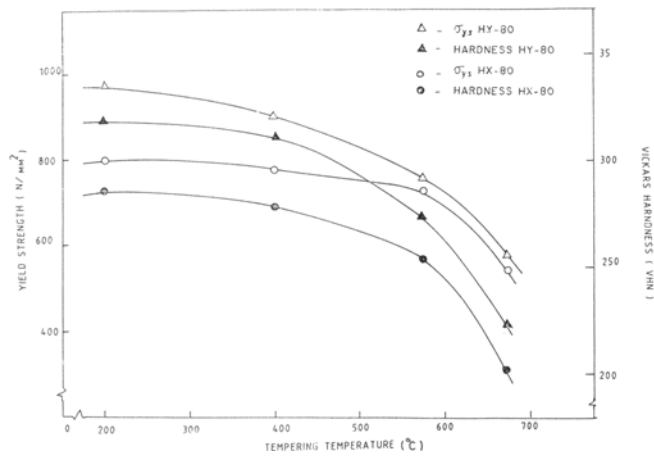


Fig. 1 Variation of yield strength and hardness with tempering temperature of HY-80 and HX-80 steels.

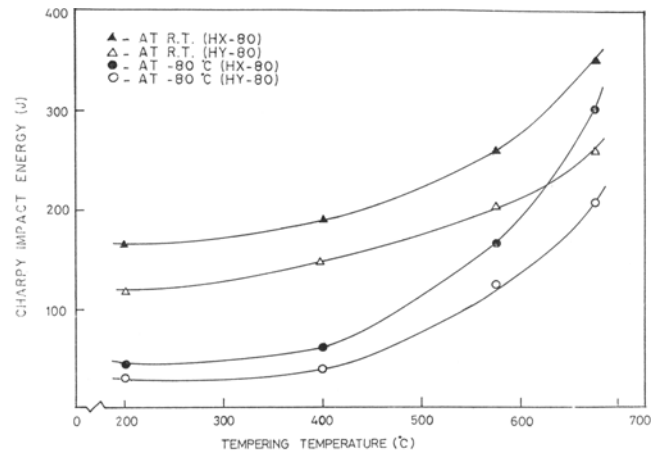
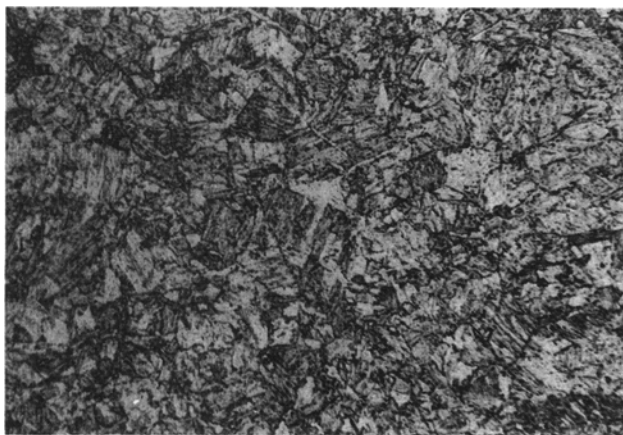
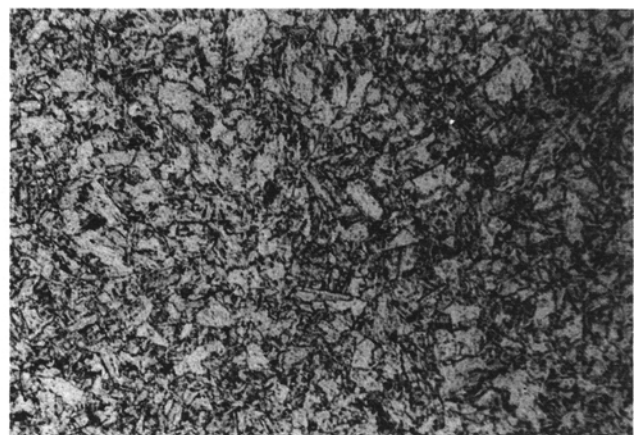


Fig. 2 Variation of Charpy impact energy with tempering temperature of HY-80 and HX-80 steels.



(a)



(b)

Fig. 3 Optical micrographs of (a) HY-80 and (b) HX-80 steels tempered at 675 °C for 1 h. 200×

and HY-80 steels. Samples for TEM analysis were prepared by the window technique to minimize the specimen volume and consequently to reduce the magnetic interaction between the lenses and the sample. An electrolyte of perchloric acid and methanol maintained at -30°C was used for thinning. A polishing voltage of 20 V was maintained.

3. Results

3.1 Mechanical Properties

The mechanical properties, namely, hardness, yield strength, and Charpy impact energy, of HX-80 and HY-80 steels are plotted in Fig. 1 and 2. Typical of low plain-carbon steels, hardness and yield strength decreased with increasing tempering temperature, whereas toughness increased. Although the change in mechanical properties with tempering temperature of both HY-80 and HX-80 steel was similar, HY-80 steel exhibited a higher yield strength than the HX-80 steel in the range of the tempering temperature up to 575 °C.

3.2 Optical Metallography

Figures 3(a) and (b) show typical optical micrographs of HY-80 and HX-80 steel tempered at 675 °C. The prior austenite grain size of HX-80 was found to be 4 to 5 μm and that of HY-80 was 7 μm . The photomicrographs illustrate the typical tempered martensitic structure for both steels.

3.3 Transmission Electron Microscopy

Some salient microstructural features of both HY-80 and HX-80 steels in the as-quenched samples and also in the tempered samples are discussed below, with emphasis on their essential differences.

3.3.1 As-Quenched Alloys

Figures 4(a) and (b) show the typical lath morphology of the martensite in both the HY-80 and HX-80 steel, in which martensite laths are stacked in near parallel array within the packets. As confirmed by selected area diffraction (SAD) pat-

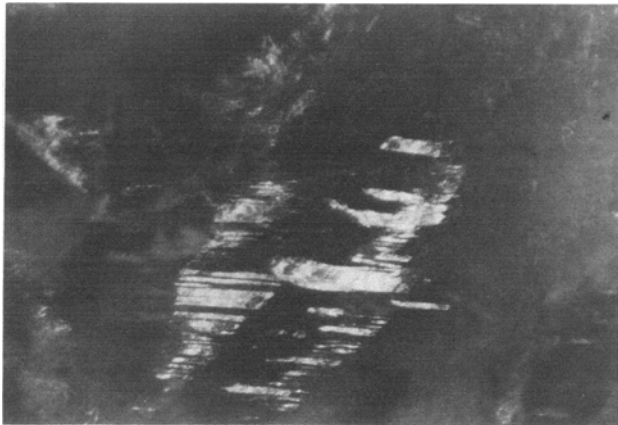


(a)

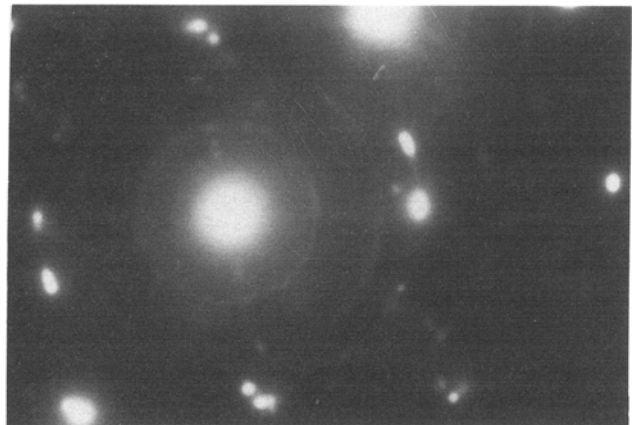


(b)

Fig. 4 Electron micrographs of (a) HY-80 (12,000 \times) and (b) HX-80 (50,000 \times) steels in the as-quenched condition.



(a)



(b)

Fig. 5 Electron micrograph of HY-80 steel showing (a) twinning (60,000 \times) and (b) SAD analysis of the area.

terns, several packets (each of which corresponds to one of the crystallographic variants of the orientation relationship between the austenite and martensite) made up the entire volume of the prior austenite grains. It has been well established^[3,4] that there are 12 such possible orientation relationships between austenite and martensite phases. The laths terminated at packet boundaries where two groups of laths belonging to two distinct orientations met. The lath width was about 0.3 μm in both the steels.

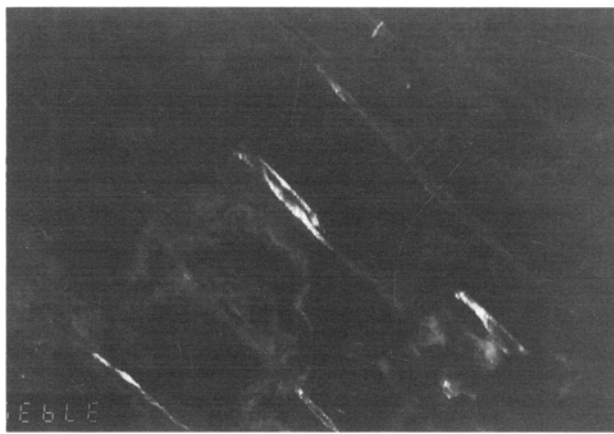
Although the lath boundary structure was not resolved, it was confirmed from electron diffraction measurements that the lath boundaries did not contain any untransformed austenite. The absence of retained austenite in both the HX-80 and HY-80 steel was confirmed by X-ray diffraction measurements. Because of the absence of retained austenite in the microstructure, the orientation relationship between austenite and martensite was not established. The TEM microstructure also revealed a small amount of twinning (<5%) in the martensitic microstructure of HY-80 steel (Fig. 5a), whereas no twinning was ob-

served in the as-quenched HX-80 samples. Analysis of the SAD pattern obtained from the bright field (Fig. 5b) confirmed that these were well known [112] microtwins. Further examination by TEM of both the HY-80 and HX-80 samples revealed very high dislocation density in the laths (Fig. 4a and b).

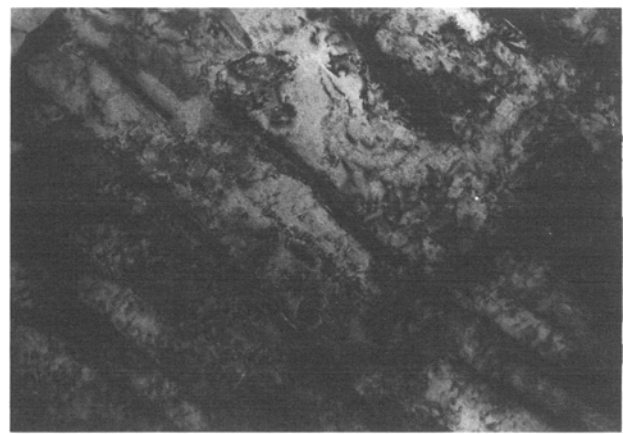
3.3.2 Structure of Tempered Alloys

In the as-quenched structure, no significant differences were observed in the microstructural features of tempered alloys of HX-80 or HY-80 steel, except the number of carbide particles. Both the steels exhibited essentially similar microstructural features. However, some differences in terms of carbide distribution were noticeable. These are described below.

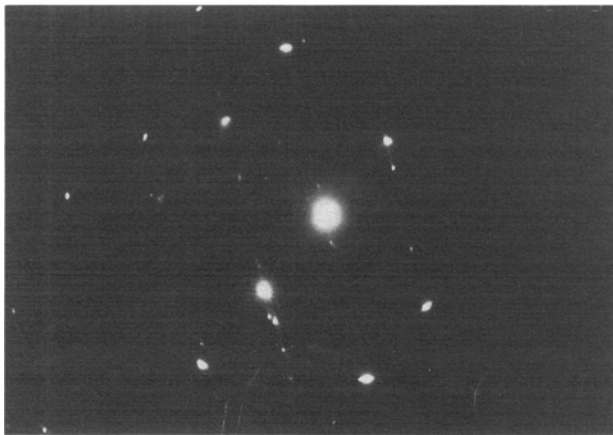
Tempering at 200 $^{\circ}\text{C}$ resulted in well-established [110] rod-shaped cementite platelets in both steels at interlath boundaries. Figures 6(a) and (b) consist of bright- and dark-field electron micrographs of HX-80 steel tempered at 200 $^{\circ}\text{C}$, revealing interlath cementite precipitation. Figure 6(c) is the



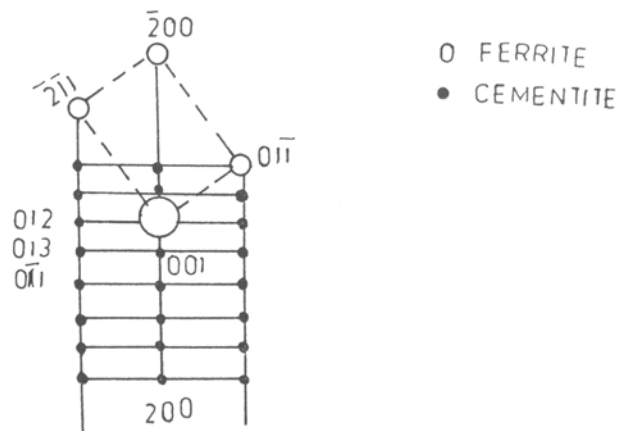
(a)



(b)



(c)



(d)

Fig. 6 Electron micrograph of HX-80 steel tempered at 200 °C for 1 h. (a) Bright field (37,000×). (b) Dark field (37,000×). (c) SAD analysis. (d) Schematic representation. Open symbols, ferrite; closed symbols, cementite.

SAD analysis of this area, and Fig. 6(d) is its schematic representation identifying the carbide as cementite. The beginning of spheroidizing of interlath cementite particles and formation of fine carbide precipitates in the early stage are evident in alloys tempered at 400 °C (Fig. 7a and b). At 575 °C, the rod-shaped carbides dissolved, and spheroidal Fe₃C formed, the later being favored by reduction in surface energy and possibly chemical energy. The spheroidal carbide particles nucleated primarily at the lath boundaries and prior austenitic grain boundaries, although some matrix nucleation was also evident.

Further examination of samples tempered at 575 °C revealed that the microstructure contained dislocation arrays. This suggested that recovery of dislocation structure occurred during tempering at 575 °C, resulting in a decrease of dislocation density and in the formation of regular array of dislocations in the ferrite matrix. The martensitic lath structure was still persistent at this temperature in both the steels. This tempering treatment also resulted in coarsening of carbide particles to an average size of 1 μm. The growth of particles occurred by dissolution of fine carbide particles. Figures 8(a) and (b) consist of bright- and dark-field electron micrographs of HX-80

and HY-80 steels tempered at 575 °C, revealing the presence of spheroidized cementite particles, and Fig. 8(c) is a SAD analysis of the area, with Fig. 8(d) providing a schematic representation identifying the carbide as cementite.

The microstructure of steels tempered at 675 °C exhibited considerable spheroidization of cementite. Also, the martensitic lath boundaries were curved, indicating the onset of recrystallization (Fig. 9a and b). The dislocation density at 675 °C for HX-80 and HY-80 are in the range of 10¹¹ to 10¹² dislocations per cm². The dislocation density was determined using the formula given by Smallman:^[5]

$$P = 1/t (n_1/l_1 + n_2/l_2)$$

where P is the dislocation density in cm⁻²; t is foil thickness; n_1 and n_2 are the number of intercepts a dislocation makes on a line of length L drawn on the micrograph; and l_1 and l_2 are the length of orthogonal lines.

The average diameters of the carbide particles tempered at 575 and 675 °C revealed that there was a wide variation in the measured diameters of the tempered carbides in both the steels



(a)



(b)

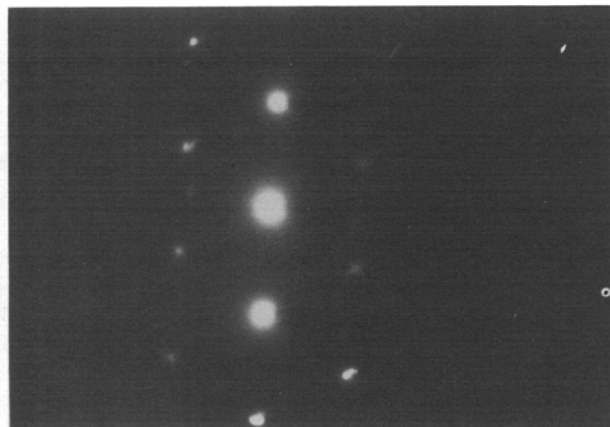
Fig. 7 Electron micrograph of (a) HY-80 (50,000 \times) and (b) HX-80 (21,000 \times) steels tempered at 400 $^{\circ}$ C for 1 h.



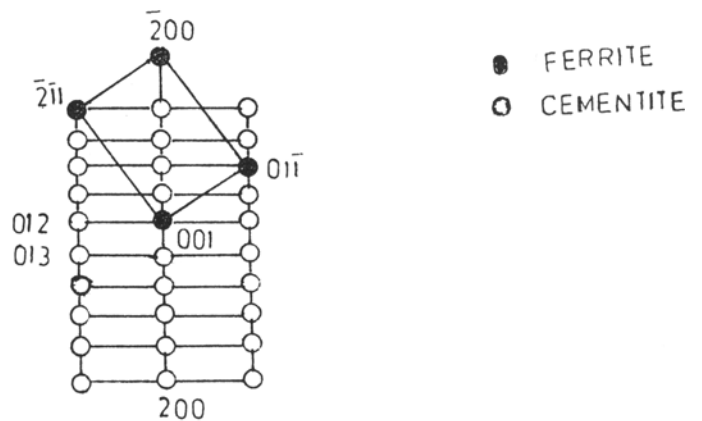
(a)



(b)



(c)

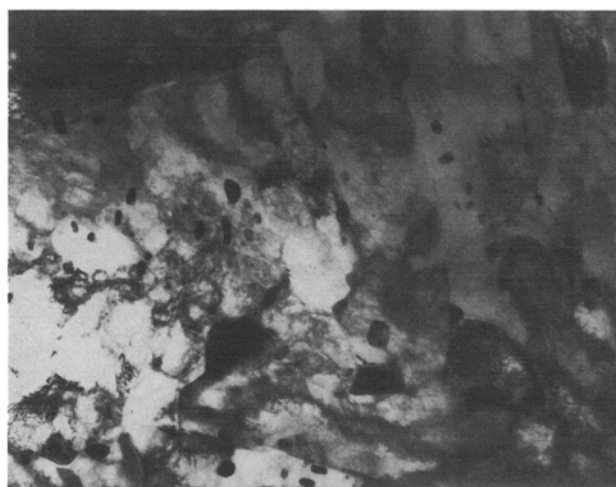


(d)

Fig. 8 Electron micrograph of HY-80 and HX-80 steels tempered at 575 $^{\circ}$ C for 1 h. (a) Bright-field micrograph of HY-80 steel (50,000 \times). (b) Bright-field micrograph of HX-80 steel (50,000 \times). (c) SAD of HX-80 steel. (d) Schematic representation. Open symbols, cementite; closed symbols, ferrite.



(a)



(b)

Fig. 9 Electron micrograph of HY-80 (a) and HX-80 (b) steels tempered at 675 °C for 1 h.

(0.2 to 2 μm). However, the density of the particles was less in HX-80 steel compared to HY-80 steel. In the HY-80 steel, a higher density of carbide particles existed both at the interlath as well as at the intralath martensite. This feature was persistent at all tempering temperatures.

4. Discussion

HY-80 steel is generally used in commercial practice at a strength level of ~ 550 MPa, which is obtained by tempering at 675 °C. This strength level in HX-80 steel can be achieved only by judicious selection of tempering temperature. From Fig. 1, it is evident that HX-80 is tempered at 650 °C, 25 °C below that used for HY-80 steel to achieve comparable strength and toughness. However, the superior toughness properties of HX-80 steel (Fig. 2), albeit being tempered at a lower temperature, is attributed to lower carbon content and finer grain size. The tempering behavior and strengthening mechanism of HX-80 and HY-80 steels at various tempering temperatures are discussed in the paragraphs below in terms of microstructural and compositional parameters.

The strengthening of martensite has been studied in several investigations, and it was shown that the strength of martensite arises from two factors: (1) structural contribution and (2) carbon content. Speich and Wartimont^[6] developed the following equation for the quantitative estimation of yield strength from carbon content:

$$\sigma_{ys} (0.2\%, 1000 \text{ lb/in.}^2) = 60 + 250 (\text{wt}\% \text{ C})^{1/2}$$

This equation was determined from low-carbon iron-carbon alloys containing up to 0.2% C and also fits data for martensitic steels containing 0.08 to 0.24% C and 0.4 to 0.5% Mn.^[7] The first term in the equation represents the structural contribution to strength, which includes grain size, packet size, lath width, dislocation density, etc., which is relatively constant as a func-

tion of carbon content. The second term shows the strong effect of carbon on yield strength.

The difference in strength levels of HY-80 and HX-80 steels can now be explained using the above functional relationship between carbon content and yield strength. Both the steels exhibit a similar substructure of martensite like lath width, dislocation, density, etc., which implies that the structural contribution to the strength is almost constant. It follows then that the difference in yield strength is due to the higher carbon content in HY-80 steel. Furthermore, the higher alloying content in HY-80 steel might also contribute to strength by solid-solution strengthening, although their effect is comparatively less than strengthening due to carbon.

It can be argued that comparatively finer grain size in HX-80 steel might permit additional contribution to the strength of this steel. However, as seen from the above equation, the effect on yield strength due to this structural contribution parameter is small and therefore not sufficient to offset the increase in yield strength of HY-80 steel due to carbon content.

Although the heat treatment given to both steels was the same, HX-80 steel exhibited comparatively finer grain size than HY-80 steel. This could be due to the presence of microalloying elements such as niobium and vanadium in the form of carbides and/or carbonitrides. The presence of microalloying carbides was not determined, because it involves tedious analytical electron microscopy or chemical extraction methods. However, the presence of vanadium or niobium in the steel was confirmed by repeat chemical analysis of the sample. It is well documented by several investigators that niobium and vanadium can bring about a very high degree of grain refinement by grain boundary pinning.^[8,9] It was also reported that a small addition of copper, which is present as a residual element in this steel, promotes the formation of very fine interalloyed precipitation of carbides or carbonitrides in the presence of niobium and/or vanadium.^[10]

Above 575 °C, rod-shaped carbides have spheroidized and resulted in the formation of equiaxed ferrite grains in both the

steels, and therefore, strength decreased thereafter because the substructure strengthening component disappeared. At this stage, the difference in yield strength between HY-80 and HX-80 steels was only marginal. This is reasonable because the ferrite structure is similar in both steels, and the spheroidal carbides are too widely spaced to cause significant strengthening by carbide dislocation interaction.^[11]

5. Conclusions

Microstructural characterization of two HSLA steels, namely HY-80 and HX-80, showed that there were no significant differences in the morphological features such as lath size and width in both quenched as well as in the tempered conditions. The density of cementites was greater for HY-80 than for HX-80 steels. The major factors contributing to the equivalent strength, superior toughness, and weldability of HX-80 steel compared to HY-80 steel are controlled tempering, lower carbon content, and finer grain size.

Acknowledgments

The authors wish to thank Dr. P.C. Deb, Director, NCML, Bombay, for his continued support and encouragement of this

research and for his permission to publish this paper. The authors also thank the authorities of BARC, Bombay, and BHU, Varanasi, for extending the use of the TEM facilities.

References

1. F. Matsuda, N. Nakaguwa, and K. Shinozaki, IIW Doc. IX-1403-86, 1986, p 1.
2. I. Lemay, L.M.D. Schety, and M.R. Krishnadev, *Proc. Int. Conf. HSLA Steels*, D.P. Dunne and T. Chandra, Ed., American Society for Metals, Aug 20-24, 1984, p 64.
3. G.R. Speich and P.R. Swan, *J. Iron Steel Inst., London*, Vol 203, 1965, p 480.
4. J.M. Chilton, R.J. Barton, and G.R. Speich, *J. Iron Steel Inst., London*, Vol 208, 1970, p 184.
5. R.E. Smallman and K.H.G. Ashbee, in *Modern Metallography*, Pergamon Press, 1966, p 184.
6. G.R. Speich and H. Wartimont, *J. Iron Steel Inst., London*, Vol 206, 1968, p 385.
7. W.H. Farland, *Trans. TMS-AIME*, Vol 233, 1967, p 20.
8. R.A. Depaul and A.L. Kitchen, *Metall. Trans.*, Vol 1, 1970, p 389.
9. P.P. Hydren, A.L. Kitchen, and P.W. Schaller, *Metall. Trans.*, Vol 2, 1971, p 2541.
10. M.L. Lafrance, F.A. Caron, G.R. Lamant, and J. Laclere, in *Microalloying-75*, 1975, p 367.
11. G.R. Speich and W.C. Leslie, *Metall. Trans.*, Vol 3, 1972, p 1043.